

Title	Formation of Metastable Phase in Vapor-Deposited FeSb Films
Author(s)	Shigematsu, Toshihiko; Shinjo, Teruya; Bando, Yoshichika; Takada, Toshio
Citation	Bulletin of the Institute for Chemical Research, Kyoto University (1979), 57(4): 310-317
Issue Date	1979-10-15
URL	<a href="http://hdl.handle.net/2433/76840">http://hdl.handle.net/2433/76840</a>
Right	
Type	Departmental Bulletin Paper
Textversion	publisher

## Formation of Metastable Phase in Vapor-Deposited FeSb Films

Toshihiko SHIGEMATSU\*, Teruya SHINJO\*,  
Yoshichika BANDO\*\*, and Toshio TAKADA\*

Received July 9, 1979

FeSb alloy films with various compositions were produced by simultaneous vapor depositions of Fe and Sb onto acetylcellulose sheets at room temperature. By electron diffraction and Mössbauer effect measurements, it was identified that 0~34 at% Sb is bcc alloy and 52~90 at% Sb is amorphous. In the supersaturated bcc alloys, the Mössbauer line width increases significantly with increasing Sb content. The amorphous alloys were stable up to about 405 K and they transformed to crystalline phases such as Fe<sub>3</sub>Sb<sub>2</sub> and FeSb<sub>2</sub>. The magnetic properties of the amorphous alloys are reported here.

KEY WORDS: Electron diffraction / Mössbauer effect / Magnetic property /  
Stability of metastable phase /

### INTRODUCTION

Metastable alloy films such as supersaturated solid solution and amorphous alloy can be produced by simultaneous vapor depositions of two components onto cold substrates. Several binary systems have been investigated, for example, supersaturated solid solutions of Cu-Co,<sup>1)</sup> Fe-Cu<sup>2,3)</sup> and Cu-Mg,<sup>1)</sup> and amorphous metallic alloys of Co-Ag,<sup>1)</sup> Fe-Au,<sup>4)</sup> and Fe-Si<sup>5)</sup> and many interesting properties were observed which differ greatly from the bulk properties.

Mader *et al.*<sup>6)</sup> classified the metastable phases obtained in the co-deposited alloy films into the following three types.

- 1) Amorphous phases may be produced when the two metals are normally insoluble in each other and the atomic size difference is large.
- 2) The co-deposited alloy films consist of ultra fine grains with the same crystal structure as that of the stable phase; in this case also diffuse halos are shown in their diffraction patterns.
- 3) The extension of the solid solution range, namely supersaturation.

If the co-deposited films show diffuse halos in their diffraction patterns, it is difficult to distinguish the Type 1) from 2). Mössbauer effect is well suited to the study of local atomic and electronic structure of alloys. Both crystallographic and magnetic properties of co-deposited alloy films will be elucidated by Mössbauer spectroscopic studies.

In this report, the results on the system of Fe-Sb are described. The equilibrium

\* 重松利彦, 新庄輝也, 高田利夫: Laboratory of Solid State Chemistry, Institute for Chemical Research, Kyoto University, Uji, Kyoto 611.

\*\* 坂東尚周: Facility for Inorganic Synthesis, Institute for Chemical Research, Kyoto University, Uji, Kyoto 611.

solubilities are limited (Sb in Fe is about 4 at% and Fe in Sb is practically nil<sup>7)</sup>). The atomic size difference is fairly large (Fe: 1.25 Å and Sb: 1.59 Å). Therefore, the appearance of the metastable phases in co-deposited alloy films is expected. In the present study, using the electron diffraction, Mössbauer effect, magnetic susceptibility and electrical resistivity measurements, metastable phases in FeSb co-deposited alloy films are detected and the magnetic properties are investigated.

### EXPERIMENTAL PROCEDURE

The films with thicknesses of 400~900 Å were prepared by simultaneous depositions of Fe (purity 99.9%) and Sb (purity 99.999%). The deposition sources on tungsten boats are heated separately and deposited onto an acetylcellulose sheets maintained at room temperature. The vacuum during the deposition was in the order of  $10^{-6}$  torr. The deposition rate of 1~5 Å/s was checked with quartz crystal thickness monitor and was constant during the deposition-run within a few percent. The film composition was determined as follows. The films were dissolved into 3~4 M hydrochloric acid and the concentrations of iron and antimony were measured by atomic absorption spectrometry.

For the electron diffraction measurements, the acetyl-cellulose sheets were removed by methyl acetate and then the films were examine by JEM-7 electron microscope.

Mössbauer effect measurements were made using a conventional spectrometer. <sup>57</sup>Co diffused in copper plate was used as a source. The velocity scale was calibrated by using an iron foil as the standard absorber.

The electrical resistivity measurements were carried out from 2 K to 300 K by means of the usual four-point method using a dc potentiometer.

Magnetic susceptibility and magnetization were measured between 4.2 K and 300 K with a magnetic torsion balance. Those measurements were made after removing the acetylcellulose in order to avoid the diamagnetic contribution.

Aging behavior of these alloy films was also studied by using Mössbauer effect. The alloy films were sealed in evacuated pyrex tubes and annealed at different temperatures for 30 minutes.

### RESULTS AND DISCUSSION

From electron diffraction measurements, the obtained films were classified into four groups. Alloys with up to 34 at%Sb concentration had bcc structure and alloys with 52~90 at%Sb had amorphous structure. While, alloys with 34~52 at%Sb were mixture of bcc solid solution and amorphous alloy, and those with 90~100 at%Sb were also mixture of amorphous alloy and Sb. No effect of deposition rate on the formation of alloy phases was observed in this experiment. Figure 1 shows typical electron diffraction patterns for FeSb alloy films.

The <sup>57</sup>Fe Mössbauer spectra at 295 K for FeSb alloy films with 4, 17, and 28 at%Sb shown in Fig. 2 are examples of those observed for the bcc phase. The line intensity ratio of nearly 3:4:1 in each hyperfine spectrum indicates that the magnetization lies in the film plane. The line width increases significantly with increasing

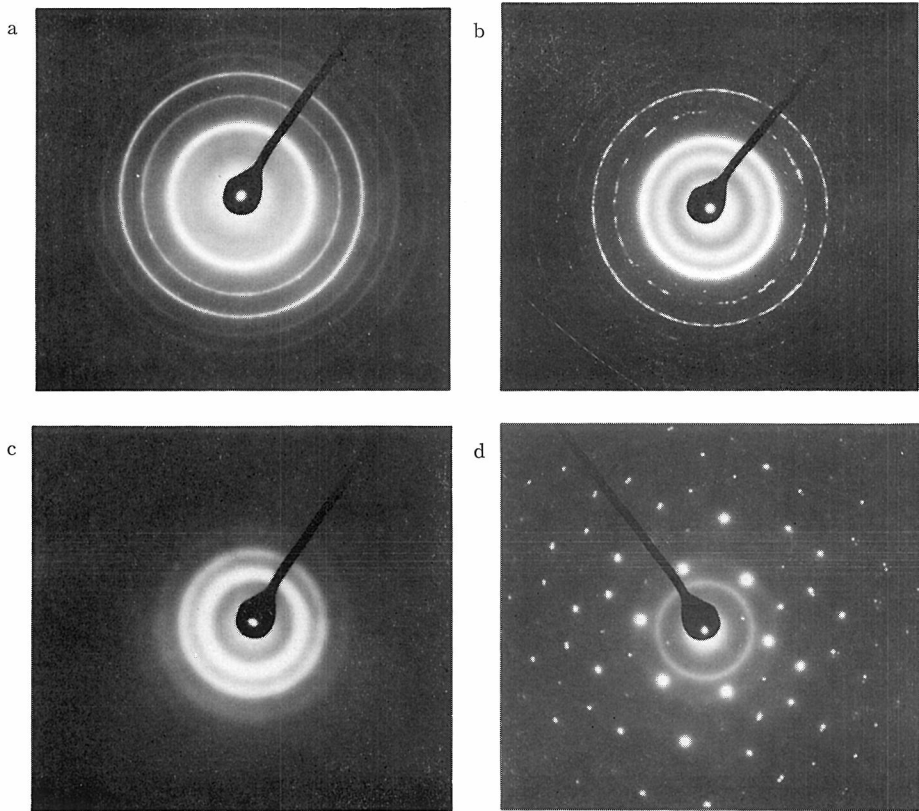


Fig. 1. Electron diffraction patterns of FeSb co-deposited films: (a) bcc phase; (b) mixture of bcc and amorphous phase; (c) amorphous phase; (d) mixture of amorphous phase and Sb.

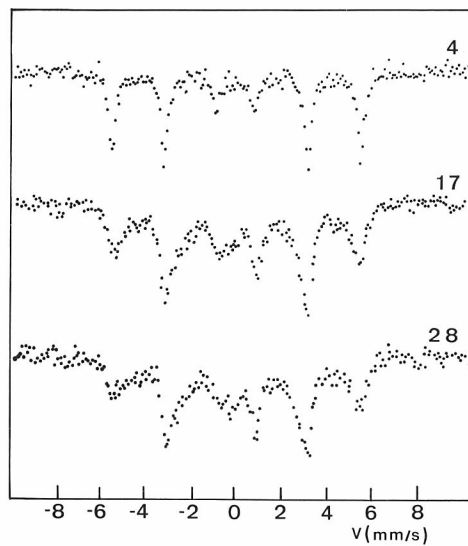


Fig. 2. Mössbauer spectra of bcc  $\text{Fe}_{100-x}\text{Sb}_x$  films at 295 K.

Sb content. Since the broadening of the outer lines are the most remarkable, the distribution of the hyperfine field should be the main reason of the broadenings. The hyperfine field of Fe depends on the number of Sb neighbors and their configurations. It is reasonable that the distribution becomes wider with increasing of Sb concentration. The mean hyperfine field at 295 K decreases with increasing Sb content, namely 330, 311, and 300 kOe for alloys with 4, 17, and 28 at% Sb, respectively. These facts indicate that a high degree of atomic cluster formation, observed in co-deposited FeCu alloy films,<sup>3)</sup> does not occur in these alloy films. Sb atoms may be solved randomly in iron matrix.

The central broad doublet line observed in the spectra of 17 and 28 at% Sb is due to the oxidized fraction. At 4.2 K, these oxide phases show magnetic hyperfine spectra. The observed Mössbauer parameters, I.S. (vs  $\alpha$ -Fe)=0.32 mm/s,  $\Delta E$ =1.10 mm/s and FWHM=1.00 mm/s at 295 K and  $\bar{H}$  (mean hyperfine field)=480 kOe at 4.2 K are similar to those observed in amorphous iron (III) oxide films obtained by reactive evaporation method.<sup>8)</sup>

After aging the specimen of Fe<sub>83</sub>Sb<sub>17</sub> for 1 hour at 530 K, no remarkable change was observed in the Mössbauer spectra, indicating that the most of the iron atoms remained in the metastable bcc FeSb alloy and the local Sb configuration around the Fe atoms was the same as those in the as-deposited alloy. After aging the same specimen at 580 K for 1 hour, the proportion of oxide phase increased and a part of it shows magnetic hyperfine structure even at 295 K. Because of the oxide formation and grain growth of the oxide phase after aging at higher temperatures, Mössbauer spectrum becomes very complicated. It is difficult to know the segregation-start temperature and what phase is obtained after aging.

The Mössbauer spectra at 295 K for FeSb alloy films with 38 and 44 at% Sb are shown in Fig. 3. In the spectra, a quadrupole splitting paramagnetic doublet due to amorphous phase is superposed to broad 6-line spectra. Based on the integrated intensities of the two patterns, 82% and 50% of the iron atoms are contained in the bcc phase in the Fe<sub>62</sub>Sb<sub>38</sub> and Fe<sub>56</sub>Sb<sub>44</sub>, respectively. We may assume here that the solubility of Sb into bcc phase is the same in these two alloys and also the composition of amorphous phase is the same. We can thus estimate the solubility limit of Sb in bcc phase and concentration of amorphous phase from these results. Then, solubility limit of Sb in bcc phase is obtained as 34 at% Sb and alloys above 52 at% Sb are amorphous phase.

The Mössbauer spectra at 295 K for FeSb alloy films with 53, 68, 77, and 90 at% Sb shown in Fig. 4 are typical of those observed for amorphous alloys. Mössbauer spectra show a well-resolved quadrupole splitting at 295 K, except for the case of 53 at% Sb<sup>9)</sup>. The values of I.S. and  $\Delta E$  were 0.42 mm/s and 0.43 mm/s at 295 K independently of Sb content. In the case of 53 at% Sb, the Mössbauer spectrum was formed by two doublets. The major one has similar I.S. and  $\Delta E$  as those of the films with compositions more than 62 at% Sb. The minor one has a larger  $\Delta E$  (0.84 mm/s) and a smaller I.S. (0.37 mm/s), which means higher  $d$  electron density than the major part. The alloys Fe<sub>23</sub>Sb<sub>77</sub> and Fe<sub>10</sub>Sb<sub>90</sub> are Pauli paramagnetic with almost temperature independent susceptibilities ( $\chi=28 \times 10^{-6}$  emu/g and  $12 \times 10^{-6}$

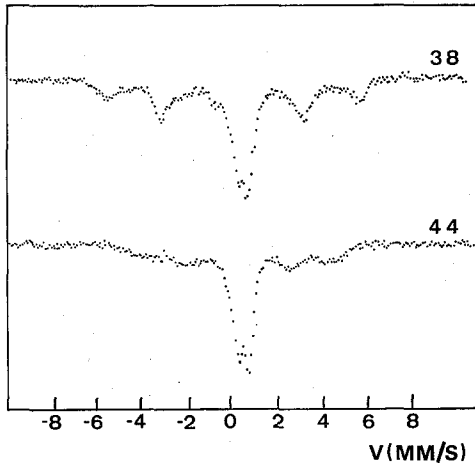


Fig. 3. Mössbauer spectra of  $\text{Fe}_{100-x}\text{Sb}_x$  alloy films at 295 K. These films are mixture of bcc and amorphous phase.

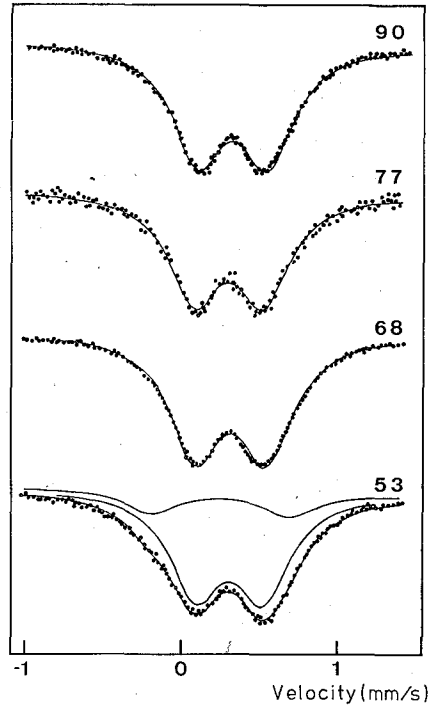


Fig. 4. Mössbauer spectra of amorphous  $\text{Fe}_{100-x}\text{Sb}_x$  films at 295 K.

emu/g, respectively). All the other alloys which have more Fe content show a magnetization which increases with decreasing temperature. Figure 5 shows the temperature dependence of magnetization. At 4.2 K, the Mössbauer spectrum of  $\text{Fe}_{47}\text{Sb}_{53}$  shows unresolved magnetic hyperfine splitting which is superposed to the central quadrupole doublet as is shown in Fig. 6. While, the Mössbauer spectra at 4.2 K

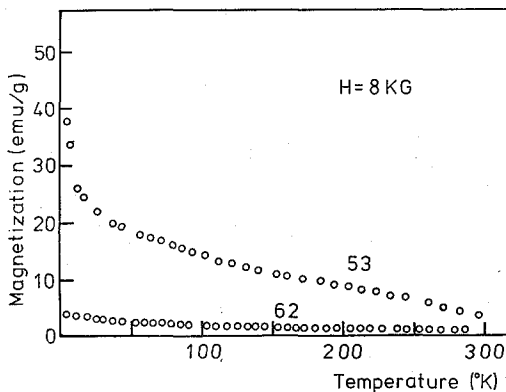


Fig. 5. Temperature dependence of the magnetization in amorphous  $\text{Fe}_{100-x}\text{Sb}_x$  films.

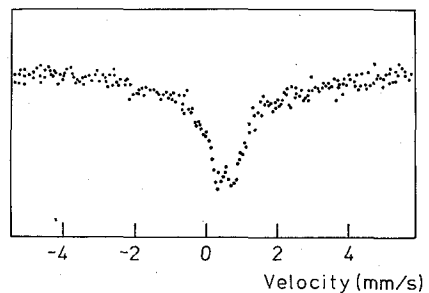


Fig. 6. Mössbauer spectra of amorphous  $\text{Fe}_{47}\text{Sb}_{53}$  film at 4.2 K.

for 68, 77, and 90 at% Sb show only a quadrupole doublet. From these results, we may conclude that Fe atoms in amorphous alloys of 68, 77, and 90 at% Sb do not carry a magnetic moment. Only a few Fe atoms which have many Fe nearest neighbor atoms can bear a magnetic moment.

All amorphous alloys investigated here have a high electrical resistivity with a very low temperature coefficient. The value and temperature coefficient of electrical resistivity obtained in this experiment change remarkably with the film thickness. It is difficult to obtain a concentration dependence of the value of electrical resistivity. Experimental results for  $\text{Fe}_{23}\text{Sb}_{77}$  with thickness of 720 Å and  $\text{Fe}_{32}\text{Sb}_{68}$  with 440 Å shown in Fig. 7 are typical for amorphous alloy films. The values at 2.2 K are  $560 \mu\Omega\cdot\text{cm}$  for  $\text{Fe}_{23}\text{Sb}_{77}$  and  $2,446 \mu\Omega\cdot\text{cm}$  for  $\text{Fe}_{32}\text{Sb}_{68}$ . All of the films investigated here have negative temperature coefficients. These negative temperature coefficients are often observed in metallic amorphous alloys.<sup>10)</sup> These experimental results show that the amorphous alloy films obtained here have a metallic conduction.

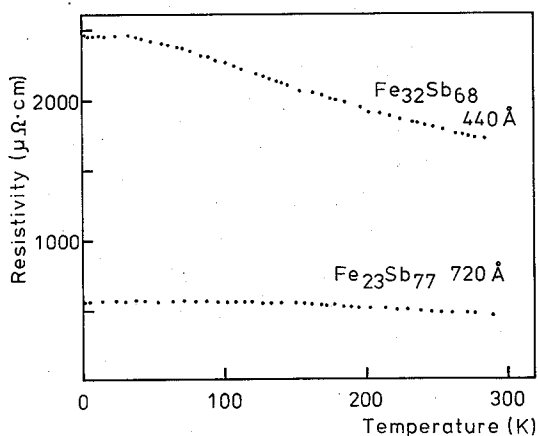


Fig. 7. Temperature dependence of the electrical resistivity of amorphous FeSb films.

Two intermetallic compounds,  $\text{Fe}_3\text{Sb}_2$  (42~48 at% Sb) and  $\text{FeSb}_2$  (66.7 at% Sb) were found in the equilibrium phase diagram of Fe-Sb system.<sup>7)</sup>  $\text{Fe}_3\text{Sb}_2$  is isomorphous with NiAs (B8 type). This compound is antiferromagnetic with  $T_N=210 \text{ K}$ .<sup>11)</sup> The observed Mössbauer parameters are I.S.=0.3 mm/s and  $\Delta E=0.3 \text{ mm/s}$  at 295 K and  $\bar{H}=100 \text{ kOe}$  at 4.2 K.  $\text{FeSb}_2$  is isomorphous with marcasite  $\text{FeS}_2$  (C18 type).  $\text{FeSb}_2$  appears to be more like a semimetal than a semiconductor.<sup>12)</sup>  $\text{FeSb}_2$  has an extremely narrow band gap ( $\sim 0.026 \text{ eV}$ ) and shows unusual electric and magnetic properties.<sup>12,13)</sup> At low temperatures ( $<80 \text{ K}$ ), the electrons are in the  $d^4$  low spin state and  $\text{FeSb}_2$  is diamagnetic. As the temperature increases, a partial unpairing of the 3d electrons due to promotion to the conduction band occurs and magnetic susceptibility increased with increasing temperature. Above 280 K, van Vleck temperature independent paramagnetism ( $\chi=1.8 \times 10^{-6} \text{ emu/g}$ ) is observed. The observed Mössbauer parameters are I.S.=0.450 mm/s and  $\Delta E=1.268 \text{ mm/s}$  at 296 K.<sup>13)</sup> From the comparison of the magnetic and electrical properties of amorphous

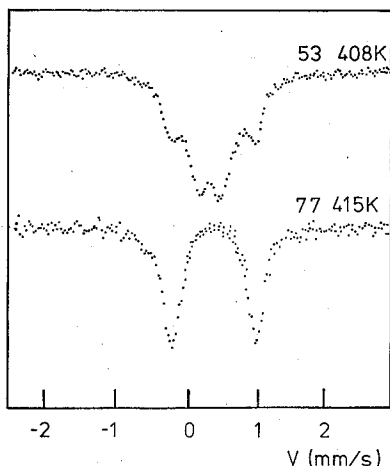


Fig. 8. Mössbauer spectra of  $\text{Fe}_{47}\text{Sb}_{53}$  and  $\text{Fe}_{23}\text{Sb}_{77}$  films after crystallization.

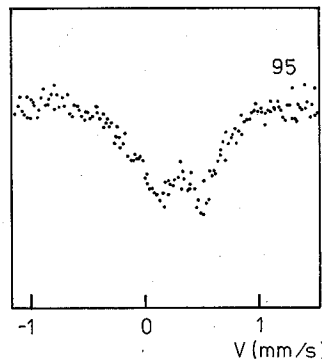


Fig. 9. Mössbauer spectrum of  $\text{Fe}_5\text{Sb}_{95}$  at 295 K. This film is a mixture of amorphous phase and Sb.

FeSb alloys with those of the intermetallic compounds, we can conclude that amorphous FeSb alloys obtained here are not the assembly of ultrafine grains of  $\text{Fe}_3\text{Sb}_2$  and/or  $\text{FeSb}_2$ .

After aging the specimens of amorphous alloys for 30 minutes up to 365 K, no remarkable change was observed in the Mössbauer spectra. These amorphous alloys were stable for aging at 365 K. A remarkable change in the spectra occurred after aging the specimens at 408 K for 30 minutes as is shown in Fig. 8.  $\text{Fe}_{47}\text{Sb}_{53}$  changes to mixture of crystalline  $\text{Fe}_3\text{Sb}_2$  and  $\text{FeSb}_2$ . At temperatures above 408 K, crystallization takes place in amorphous FeSb alloys with 52~66.7 at% Sb. Using Mössbauer effect, it is found that both  $\text{Fe}_3\text{Sb}_2$  and  $\text{FeSb}_2$  are present after crystallization takes place. In the specimen of  $\text{Fe}_{23}\text{Sb}_{77}$  aged at 415 K for 30 minutes, only a well-resolved quadrupole splitting due to  $\text{FeSb}_2$  was observed in the spectrum (Fig. 8). From this result and the fact that the solubility of Fe in Sb is practically nil in bulk alloy, we can conclude that the amorphous alloys with 66.7~90 at% Sb crystallize to the mixture of  $\text{FeSb}_2$  and Sb after aging at above 415 K. The melting temperature ( $T_m$ ) of  $\text{Fe}_3\text{Sb}_2$  is about 1290 K and  $\text{FeSb}_2$  transforms to the mixture of  $\text{Fe}_3\text{Sb}_2$  and liquid at 1000 K. From these values we can estimate a reduced crystallization temperature  $T_c/T_m$  for amorphous FeSb alloy. These values are from 0.32 to 0.40, which are similar to those obtained in other amorphous alloys.

The Mössbauer spectrum at 295 K for FeSb alloy film with 95 at% Sb shown in Fig. 9 is typical of those observed for mixture of amorphous alloy and Sb. Mössbauer spectrum show a quadrupole splitting at 295 K. This spectrum is similar to those observed in amorphous FeSb alloys. From this spectrum, we may conclude that all of iron atoms are contained in the amorphous phase in the FeSb alloy films with 90~100 at% Sb. The solubility of Fe in Sb in co-deposited FeSb alloy films is almost nil.

Two types of metastable alloy phases, supersaturated bcc solid solution and



metallic amorphous alloy were produced in co-deposited FeSb alloy films, as described before. The supersaturated solid solution exists in the composition range of 0~34 at% Sb. From the equilibrium phase diagram,<sup>7)</sup> the solubility of Sb in  $\alpha$ -Fe is about 4 at% at room temperature and about 20 at% at 1275 K. This more extended equilibrium solid solubility at higher temperature may produce the supersaturated solid solution of 34 at% Sb. The metallic amorphous alloy exists in the composition range of 52~90 at% Sb. According to Mader,<sup>14)</sup> the factors which favor the appearance of an amorphous phase in co-deposited alloy films are a) a relatively large difference ( $\sim 10\%$ ) in the atomic radii of the components and b) the absence of an extend equilibrium solid solubility. The difference in the atomic radii of the components is 21.4% for FeSb. This fact is favorable to obtain the amorphous alloy films with wide composition range. While, the solid solubility of Sb in Fe is about 4 at% at room temperature. This leads to the rather narrow composition range, 52~90 at% Sb in co-deposited FeSb alloy films.

#### ACKNOWLEDGMENT

The authors would like to thank to Professor M. Matsui and Dr. O. Fujino for their help in the atomic absorption spectrometry.

#### REFERENCES

- (1) S. Mader, *J. Vac. Sci. Technol.*, **2**, 35 (1965).
- (2) E. Kneller, *J. Appl. Phys.*, **35**, 2210 (1964).
- (3) W. Keune, J. Lauer, and D. L. Williamson, *J. de Phys.*, **35**, C6-473 (1974).
- (4) W. Felsch, *Z. Angew. Phys.*, **29**, 217 (1970).
- (5) G. Marchal, Ph. Mangin, and Chr. Janot, *Solid State Commun.*, **18**, 739 (1976).
- (6) S. Mader, A. S. Nowick, and H. Widmer, *Acta Met.*, **15**, 203 (1967).
- (7) M. Hansen, "Constitution of Binary Alloys," 2nd ed, McGraw-Hill, New York, 1958, pp. 708-710.
- (8) T. Shigematsu, Y. Bando, and T. Takada, *J. de Phys.*, **40**, C2-153 (1979).
- (9) T. Shigematsu, T. Shinjo, Y. Bando, and T. Takada, Submitted for publication in *J. Magnetism Magn. Mat.*
- (10) K. H. J. Buschow, A. M. van Diepen, N. M. Beekmans, and J. W. M. Biesterbos, *Solid State Phys.*, **28**, 181 (1978).
- (11) F. W. Richter and K. Schmidt, *Z. Naturforsch.*, **30a**, 1621 (1975).
- (12) A. K. L. Fan, G. H. Gerald, H. Rosenthal, H. L. McKinzie, and A. Wold, *J. Solid State Chem.*, **5**, 136 (1972).
- (13) J. Steger and E. Kostiner, *J. Solid State Chem.*, **5**, 131 (1972).
- (14) S. Mader, *J. Vac. Sci. Technol.*, **7**, 175 (1970).